



Geographia Polonica
2021, Volume 94, Issue 2, pp. 237-249
<https://doi.org/10.7163/GPol.0203>



INSTITUTE OF GEOGRAPHY AND SPATIAL ORGANIZATION
POLISH ACADEMY OF SCIENCES
www.igipz.pan.pl

www.geographiapolonica.pl

UTCI AS THE NWP MODEL ALADIN (CHMI) OUTPUT – FIRST EXPERIENCES

Martin Novák^{1,2} 

¹ Czech Hydrometeorological Institute
Regional Office in Ústí nad Labem
PO Box 2, Kočkovská 2699/18, 400 11 Ústí nad Labem: Czech Republic

² Faculty of the Environment
Jan Evangelista Purkyně University
Pasteurova 3632/15, 400 96 Ústí nad Labem: Czech Republic
e-mail: martin.novak@chmi.cz

Abstract

The article includes a summary of basic information about the Universal Thermal Climate Index (UTCI) calculation by the numerical weather prediction (NWP) model ALADIN of the Czech Hydrometeorological Institute (CHMI). Examples of operational outputs for weather forecasters in the CHMI are shown in the first part of this work. The second part includes results of a comparison of computed UTCI values by ALADIN for selected place with UTCI values computed from real measured meteorological data from the same place.

Key words

numerical weather prediction • UTCI • human biometeorology • thermal comfort/discomfort • weather station • biometeorological forecast

Introduction

The thermoregulatory system is one of the key parts of a functioning human organism. Sustaining a constant core temperature of the human body is its main task. The system must constantly cope with the changing conditions of the external environment, which act on the surface of the body. Human thermal comfort can then be defined as a situation in which the thermoregulatory system maintains body

temperature with minimal energy expended (Andrade et al., 2019).

The amount of energy consumed by the thermoregulatory system depends on the difference between the surface and core temperatures of the human body. The energy balance of the body's surface, which is crucial for its temperature and its changes, is formed by the balance of heat fluxes and radiation fluxes. Knowledge of energy balance is therefore the basis for the assessment of thermal comfort / discomfort.

Therefore, when trying to describe thermal comfort, it is necessary to look for such indices that do not only address some of the external factors that determine the balance (wind chill, heat index, etc.), but we must look for complex characteristics, including in addition to air temperature, humidity and airflow also flows shortwave and longwave radiation. Such indices include, for example, the Universal Thermal Climate Index (UTCI) or the Physiological Equivalent Temperature (PET).

The UTCI is very interesting tool for a biometeorological forecasting. The index describes thermal comfort/discomfort as the concurrent effect of four basic components of the external environment – air temperature, air humidity, wind speed and radiation. The UTCI is expressed as an equivalent temperature [$^{\circ}\text{C}$] of a reference environment providing the same physiological response of a reference person as the actual environment (Błażejczyk et al., 2012).

The complex character of this index is main reason behind its difficult prediction by classical meteorological methods. Standardly measured meteorological characteristics usually enter the UTCI calculation – air temperature in 2 m, relative humidity in 2 m, wind speed in 10 m (UTCI, 2012). Unfortunately, the UTCI values show non-standard behavior at high wind speeds when they are calculated from unadjusted input data. Index values unexpectedly rise at wind speeds from 20 to 27 mps, at speeds higher than 27 mps UTCI values begin to fall very rapidly to unrealistic values (Novák, 2013). Therefore, the wind speeds at the entrance to the NWP model are adjusted in accordance with the index authors recommendation (UTCI, 2012): for wind speeds $v > 17$ mps a constant value of wind speed $v' = 17$ mps is used for UTCI computation.

An exception is the description of radiation. The authors of UTCI used mean radiant temperature to express the effect of the radiation component of the energy balance. The mean radiant temperature is a parameter that combines all longwave and shortwave radiant fluxes to a single value. It is defined

as the temperature of a surrounding black body that causes the same radiant heat fluxes as the complex radiant fluxes (Fanger, 1972). In human biometeorology the mean radiant temperature is usually calculated for a standardized standing person. Since measurements are not available on many operational meteorological stations, different models exist, ranging from simple empirical models to full radiative-transfer models, which allow modeling of radiant fluxes based on standard meteorological measurements (Gosling et al., 2014).

Measurements of the shortwave and longwave components of the radiation balance are missing at most standard meteorological stations. Simplified estimates are then needed to determine the mean radiant temperature (T_{mrt}). A simpler situation can be in the case of predictions through numerical weather prediction models. Radiation fluxes are an integral part of the calculations of numerical models. That is why the CHMI Regional Forecasting Office in Usti nad Labem asked the Numerical Weather Prediction Department (NRPD) of the Czech Hydrometeorological Institute (CHMI) for extension of the list of computed characteristics for UTCI calculation in order to develop new CHMI biometeorological forecast model. As the first step, the NRPD added the mean radiant temperature among routinely calculated outputs of the ALADIN model during 2018.

The next step was an implementation of the UTCI to the ALADIN model. The NRPD has upgraded ALADIN model (CHMI) to new non-hydrostatic version with better resolution of 2.3 km (previous version had 4.6 km) and more accurate orography description (Fig. 1). The NRPD started the new version of ALADIN model in February 2019. This version already includes an UTCI calculation and CHMI is going to use this index for i.e. improvement of current biometeorological forecasts and bioclimatological mapping of the Czech Republic and other interesting subregions such as mountains, cities and spa. The UTCI will be also used for national heat health warning system (as the part of Integrated Warnings Service System).

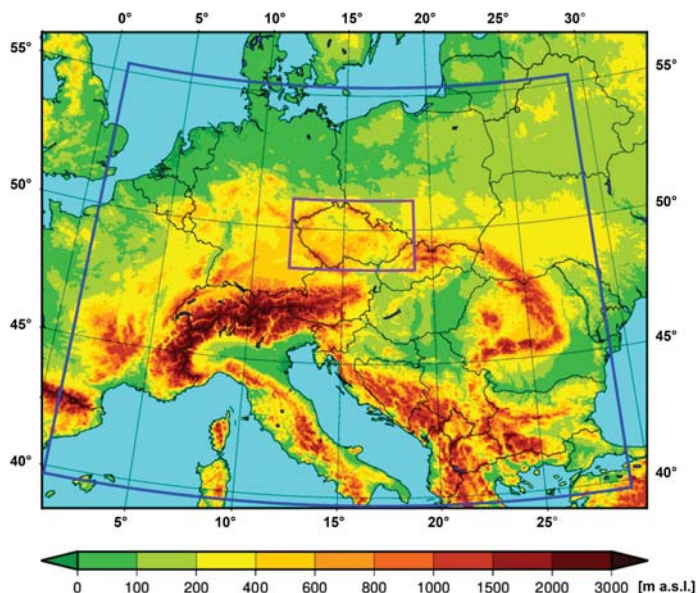


Figure 1. The area and orography of the ALADIN (CHMI) including sub-domains LL2K (blue frame) and CZ1K (purple frame)

The article is focused to an introduction of the UTCI outputs from new ALADIN model and an example of their potential using – charts, maps, tables. The comparisons with another characteristics are also possible. A simple comparison of UTCI outputs with UTCI values calculated from measured meteorological data is also presented in this article.

Data and methods

The ALADIN (Aire Limitée Adaptation dynamique Développement InterNational) System is a numerical weather prediction (NWP) system developed by the international ALADIN consortium for operational weather forecasting and research purposes. It is based on a code that is shared with the global model IFS of the ECMWF and the ARPEGE model of Météo-France (Termonia et al., 2018).

In the last 27 years, RC LACE has contributed to the limited area ALADIN system in the areas of pre-processing of observations, data assimilation, model dynamics,

physical parameterizations, meso-scale and convection permitting ensemble forecasting, and verification. It has developed strong collaborations with NWP consortia ALADIN, HIRLAM and ECMWF (Wang et al., 2018).

Diagnostics of the mean radiant temperature has been plugged into the NWP model ALADIN in the CHMI. It is defined as the temperature of a hypothetical blackbody enclosure yielding the same radiative heating as a human body at the actual shortwave and longwave fluxes. Absorption of direct sunlight is calculated assuming a rotationally symmetric human body in upright position, thus depending on sun elevation. Absorption of the shortwave and longwave diffuse fluxes is evaluated using their hemispheric mean values. Shortwave absorptivity and longwave emissivity of a human body are assumed to be 0.70 and 0.97, respectively. Instantaneous values of the mean radiant temperature are computed on the model grid at every time-step and are post-processed as required. The mean radiant temperature is a key part for UTCI calculation.

The comparison of the UTCI model values with the values calculated from the measured meteorological data was another part of this work. The values for a specific point were chosen for the first evaluation of the basic properties of the predicted UTCI values. The city automatic weather station (AWS) in Teplice (50°38'43"N, 13°50'11"E, 227 m a.s.l.) was selected to study model prediction. This standard AWS is a member of measurement network of the Czech Hydrometeorological Institute, so information on shortwave and longwave radiation is not available. Therefore, a simplified method was chosen for the UTCI calculation.

The equality $T_{mrt} = T$ is the simplest solution for calculating the UTCI value at unknown radiation fluxes for the objective calculation of T_{mrt} . This approach is used quite often, we can also find a comparison with objectively calculated values of T_{mrt} in some sources (Walikewitz et al., 2015; Chaudhuri et al., 2016). However, both of these articles work with an indoor environment. The results of other studies (Lai et al., 2017; Krüger et al., 2019) show that according to a simply calculated T_{mrt} ($T_{mrt} = T$) with an objectively determined T_{mrt} is worse in the outdoor environment. The authors record acceptable results in a shielded environment. However, large differences between the two values are manifested in the case of a clear sky, where a significant supply of shortwave radiation is manifested during the day. Deficiency of long-wave radiation then occurs at night. The differences between the real T_{mrt} and the air temperature increase in such cases.

The above-mentioned shortcomings of using $T_{mrt} = T$ led to the idea of testing another option. The fact that only a limited set of characteristics is measured at meteorological stations did not allow for a large selection. It was necessary to look among the standard measured temperature characteristics as one that responds more to radiation fluxes. This is the air temperature measured at a height of 5 cm (T_g), which responds more significantly to changes in surface temperatures. The surface temperature is very

sensitive to the balance of radiant fluxes of shortwave and longwave radiation. Therefore, T_g was chosen as an alternative value, the equality $T_{mrt} = T_g$ thus became the second tested variant.

Software Bioklima 2.6 was used to calculate UTCI (Błażejczyk et al., 2010). Statistical software R (R Core Team, 2019) was used for analyses data. The charts are made using package *ggplot2* (Wickham, 2016).

Differences between the UTCI values predicted by the ALADIN model (marked as UTCI(A)) and the values calculated from the measured data using the equality $T_{mrt} = T$ (UTCI(T), respectively $T_{mrt} = T_g$ (UTCI(T_g))) were used to verify model outputs.

Results

The mean radiant temperature (T_{mrt}) is an essential part of the UTCI equation. This characteristic has been plugged into ALADIN (CHMI) model in autumn of 2018. Then, starting in January 2019, a calculation of the UTCI was fully implemented (Fig. 2).

Two maps (Fig. 3 and 4) demonstrate a seasonal differences of the UTCI values in central Europe. The first map shows an area distribution of the UTCI values during the warmer winter noon (forecast for January 21, 2020; 12 UTC). This was winter day with temperatures above long-term normal values. Lower UTCI values in Moravia, Silesia and northern Bohemia respond to areas with predicted fogs and/or low cloudiness. Higher UTCI values are predicted for areas with forecasted sunny weather. In both parts of the Czech Republic, the air mass was the same at the time. The differences in the predicted UTCI values were thus determined almost exclusively by differences in the radiation balance. The supply of shortwave radiation was significantly suppressed in places with fog and / or low stratiform clouds. Lower T_{mrt} values result directly from this – and lower UTCI values result.

The second map (Fig. 4) shows area distribution of the UTCI values in the summer afternoon (forecast for June 30, 2019;

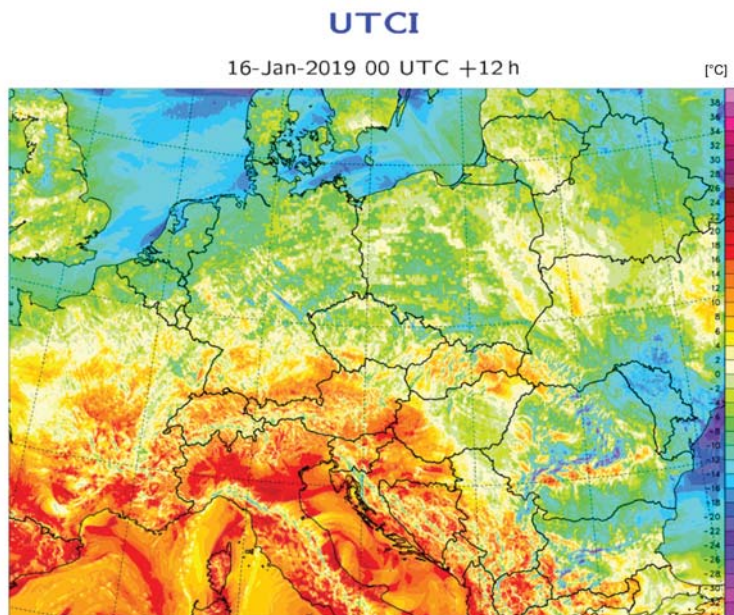


Figure 2. The first map of the UTCI forecasted by the ALADIN (CHMI) [in °C]

15 UTC) with higher values in the Bohemia with warm air-mass advection and longer sunshine. Lower values especially in Silesia and north-western Moravia are caused by clouds and a colder air-mass in these areas. In this case, the area distribution of UTCI values is not only given by the radiation balance, but air masses with different temperatures are also manifested. Warm advection from the southwest has already manifested itself in most of the Czech Republic.

A daily course of the UTCI is usually more marked than a course of air temperature. The typical course of the UTCI is illustrated by Figure 5, the colours respond to thermal stress categories (Glossary of terms for thermal physiology, 2003). The numerical forecast (from run 2019-05-17 00 UTC) for 72 hours in this table. May is typically the spring month with potentially large daily amplitudes of air temperature values. A sufficiently long time for which the Sun is above the horizon can significantly increase the values of T_{mrt} . The nights are getting shorter, but the long-wave part of the radiation

balance in dry air masses can be significantly negative. This contributes to higher daily amplitudes T_{mrt} compared to the course of air temperature. Therefore, in May, there may be both negative (cold stress) and positive (heat stress) categories of heat stress.

A “UTCI-gram” (Fig. 6) for a selected place (Teplice – spa town in NW Czechia with 50 thousands inhabitants) provides a more comprehensive overview of the links between the UTCI and other meteorological predicted values (mean radiant temperature, forecasted and measured air temperature). Most of the characteristics in the graph are predictions of the ALADIN model, the black line represents the measured air temperature at 2 m. The difference between the predicted (green line) and the measured temperature shows the tendency of the model to underestimate the real air temperatures. This fact is probably due to the urban character of the station, which is below the resolution of the model.

The graph shows the large effect of the radiation balance on UTCI in first half

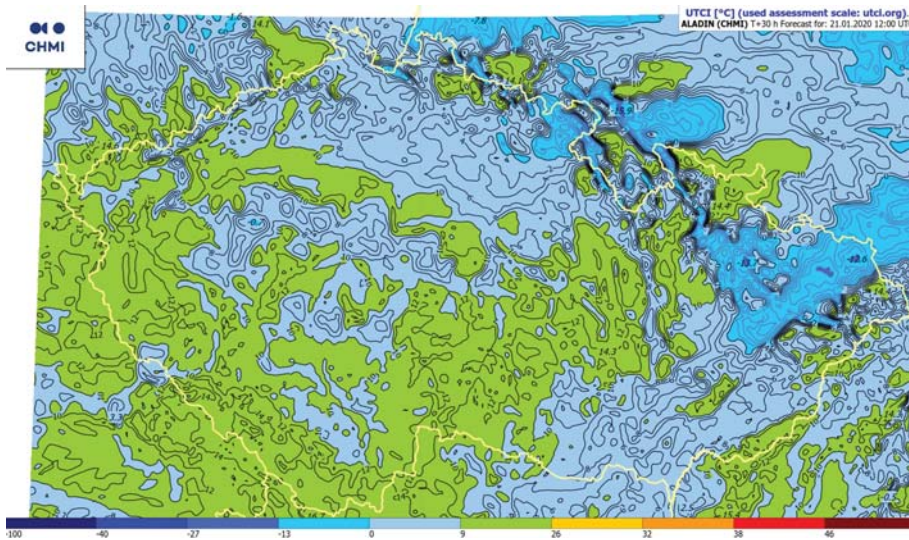


Figure 3. Example of field of the UTCI for warmer winter day (Jan 21, 2020; 12 UTC). Forecasted by the ALADIN (CHMI). Colours are in accordance with UTCI assessment scale

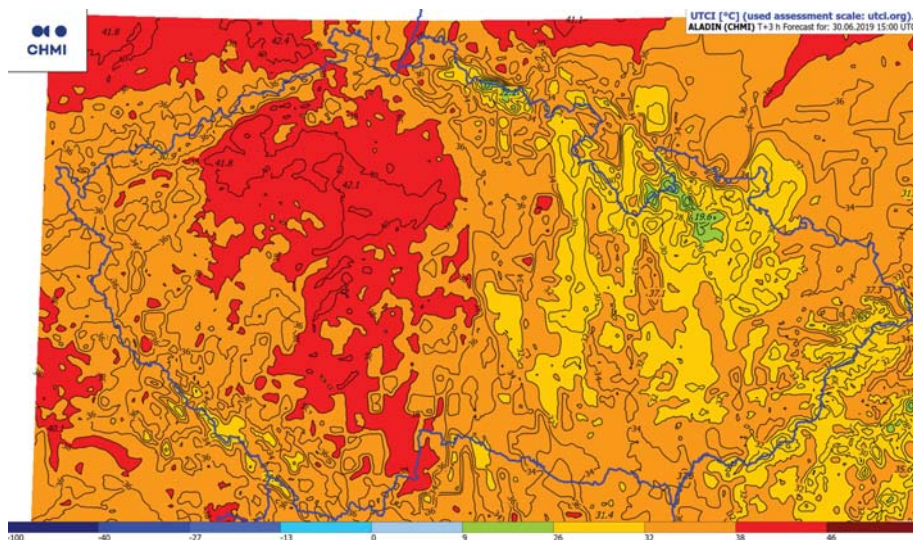


Figure 4. Example of field of the UTCI for hot summer day (Jun 30, 2019; 15 UTC). Forecasted by the ALADIN (CHMI). Colours are in accordance with UTCI assessment scale

of a period. Mean radiant temperature drops to significantly lower values than air temperature during the night with reduced clouds and with dry air-mass. The atmospheric counterradiation is more pronounced with higher absolute humidity. With a lower

amount of water vapor in the air column, the amount of longwave radiation returning to the surface is smaller, highlighting the negative radiation balance. The value of the UTCI model prediction then decreases with it. The more pronounced daily course of UTCI

| Station | Forecast for: | | | | | | | | | | | | |
|------------------|---------------|---------|---------|---------|---------|---------|---------|---------|---------|---------|---------|---------|---------|
| | +00 hrs | +06 hrs | +12 hrs | +18 hrs | +24 hrs | +30 hrs | +36 hrs | +42 hrs | +48 hrs | +54 hrs | +60 hrs | +66 hrs | +72 hrs |
| Plzeň | -3.5 | -10.8 | 1.4 | -17.2 | -22.2 | -25.1 | -16.9 | -9.8 | -18.9 | -20.4 | -7.7 | -15.9 | -22.8 |
| Karlovy Vary | -14.0 | -8.9 | -3.6 | -15.7 | -19.3 | -20.9 | -14.5 | -15.6 | -17.0 | -20.4 | -8.8 | -17.7 | -20.0 |
| České Budějovice | -7.0 | -7.3 | 10.1 | -15.1 | -14.2 | -14.5 | -1.0 | -4.6 | -19.8 | -14.0 | 2.1 | -12.8 | -12.8 |
| Teplice | -6.1 | -14.8 | 2.2 | -8.8 | -9.9 | -15.4 | -11.9 | -16.7 | -22.7 | -26.8 | -16.2 | -12.7 | -22.5 |
| Liberec | -11.3 | -13.1 | -3.9 | -21.6 | -25.6 | -24.6 | -7.3 | -16.8 | -20.1 | -11.9 | -8.7 | -11.9 | -19.1 |
| Praha, Komořany | -3.1 | -10.8 | 5.1 | -18.4 | -21.2 | -21.2 | -17.3 | -9.5 | -18.6 | -21.0 | -9.3 | -15.7 | -20.6 |
| Hradec Králové | -1.3 | -1.4 | 1.9 | -8.9 | -10.0 | -12.9 | -11.4 | -16.4 | -23.2 | -20.7 | -8.2 | -15.3 | -20.0 |
| Pardubice | -0.6 | -3.2 | 2.6 | -8.8 | -9.9 | -9.7 | -10.1 | -18.0 | -21.3 | -21.0 | -8.6 | -18.0 | -19.7 |
| Humpolec | -4.3 | -6.5 | 1.8 | -16.8 | -19.4 | -21.8 | -13.7 | -18.6 | -24.8 | -22.9 | -12.6 | -18.6 | -21.1 |
| Jihlava | -5.6 | -7.1 | 7.3 | -14.1 | -13.4 | -15.6 | -12.6 | -19.2 | -25.2 | -27.1 | -13.1 | -21.5 | -23.5 |
| Třebíč | -6.3 | -8.7 | 7.4 | -12.4 | -15.3 | -8.0 | -8.2 | -20.2 | -20.7 | -28.8 | -14.1 | -24.0 | -21.8 |
| Znojmo | -12.2 | -13.4 | 4.8 | -15.4 | -9.6 | -7.5 | -3.7 | -11.5 | -23.0 | -27.7 | -13.9 | -22.0 | -14.2 |
| Břeclav | -14.0 | -8.9 | 6.5 | -6.6 | -13.9 | -16.2 | -8.8 | -9.8 | -12.6 | -15.4 | -6.7 | -12.4 | -7.1 |
| Brno, Staré Brno | -9.8 | -7.4 | 5.4 | -11.8 | -7.4 | -10.6 | -4.0 | -6.4 | -16.9 | -18.0 | -4.7 | -11.2 | -9.5 |
| Zlín | -10.1 | -14.1 | 5.3 | -9.0 | -14.7 | -15.9 | -9.1 | -14.4 | -14.0 | -12.5 | -4.8 | -10.9 | -14.6 |
| Olomouc, Holice | -4.1 | -2.2 | 5.5 | -10.7 | -11.1 | -19.9 | -16.8 | -12.3 | -9.7 | -15.4 | -5.5 | -10.8 | -10.3 |
| Šumperk | -2.6 | -12.4 | 11.3 | -9.1 | -9.9 | -8.2 | -4.5 | -4.4 | -11.6 | -7.7 | 8.8 | -8.1 | -8.1 |
| Jeseník | -8.5 | -7.4 | 8.7 | -11.3 | -19.7 | -20.6 | -9.6 | -9.7 | -10.3 | -12.1 | -5.2 | -10.1 | -10.1 |
| Opava | -1.0 | -1.9 | 9.7 | -17.1 | -20.4 | -28.4 | -25.8 | -18.0 | -15.8 | -14.0 | -8.0 | -18.1 | -15.1 |
| Ostrava, Poruba | -2.1 | -1.7 | 8.4 | -15.8 | -23.8 | -29.3 | -22.1 | -22.0 | -9.4 | -14.3 | -9.6 | -17.0 | -20.5 |
| Rožnov p. Radh. | -10.9 | -15.2 | 10.2 | -13.0 | -15.3 | -18.3 | -10.2 | -15.6 | -10.2 | -6.0 | -7.7 | -9.2 | -11.5 |

Figure 5. The UTCI values forecasted by the ALADIN (CHMI) (Jan 11, 2021; 00 UTC) for selected places in Czechia. Colours are in accordance with UTCI Assessment scale

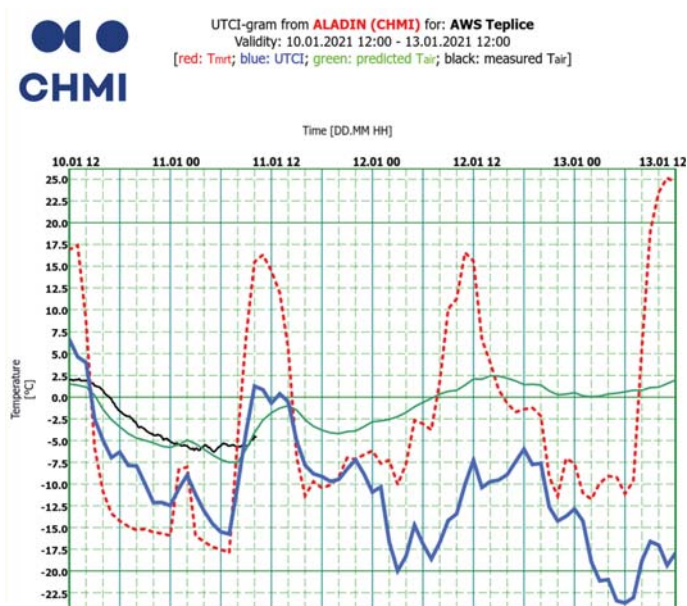


Figure 6. Values of the selected predicted thermal characteristics. Forecasted by the ALADIN (CHMI) (Jan 10, 2021; 12 UTC)

is then given by the rise of T_{mrt} in the daylight hours of sunshine.

The effect of wind speed is seen when the predicted UTCI values are decreasing below the T_{mrt} values from second half of second night. It is a situation after a pass of cold front, with cloudy skies and (mostly) higher wind speeds.

The figures with forecasts of NWP model ALADIN (CHMI) were prepared in Visual Weather environment (specialized software of IBL for meteorological services). These presented kinds of outputs are commonly available to operational meteorologists of the CHMI, mainly at Regional Forecasting Office in Ústí nad Labem. This office issues biometeorological forecasts for the Czech Republic.

Already the first data analyses showed that not only the UTCI predicted values, but also the differences between the predicted and calculated UTCI values show a significant daily course (Fig. 7 and 8). Daily run of the differences between forecasted and calculated UTCI values are described by average difference

(blue line) and median of differences (red line) for each of daily hours. Yellow line shows a standard deviation of differences. It is clear from the graphs that the model significantly underestimates UTCI at night. In daylight hours the differences decrease and especially around noon the model values are usually higher. This finding applies to both $T_{mrt} = T$ (Fig. 7) and $T_{mrt} = T_g$ (Fig. 8).

Next question after the findings of Figures 7 and 8 was obvious: the differences between the predicted and calculated UTCI values show equally pronounced daily course throughout whole year or they have seasonal fluctuations? The answers are in Figure 9 (for $T_{mrt} = T$) and 10 (for $T_{mrt} = T_g$). The graph for the whole tested period (from February to December 2019) is always the first (with the orange frame) followed by selected months from different seasons of 2019 (March for spring, July for summer and November for late autumn). A summary of the behavior of the UTCI predicted and calculated differences is shown in Figure 11. The ALADIN predicted UTCI values are generally lower than the calculated

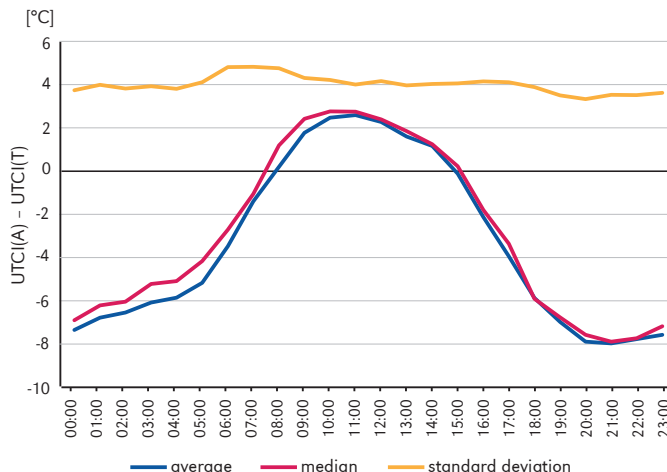


Figure 7. The daily course of differences between predicted [UTCI(A)] and calculated [UTCI(T) with $T_{mrt} = T$] UTCI values for period Feb – Dec 2019

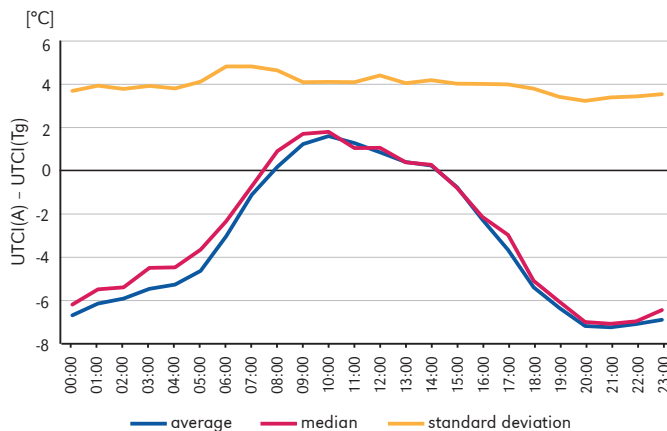


Figure 8. The daily course of differences between predicted [UTCI(A)] and calculated [UTCI(T_g) with $T_{mrt} = T_g$] UTCI values for period Feb-Dec 2019

values over the whole period. The predicted values show (insignificantly) smaller differences from the values calculated at $T_{mrt} = T_g$.

Conclusions

Operational calculation of mean radiant temperature and UTCI model of CHMI ALADIN is a great helper for everyday meteorology and biometeorology. This indicator helps

to understand the principles of the concurrent effect of basic meteorological factors affecting the radiation and heat balance of the human body surface and thus the feeling of thermal comfort or discomfort.

Tests have shown that UTCI predicted values are generally lower than those calculated from the measured data. However, this statement does not relate universally. The mutual relation of the predicted and calculated UTCI

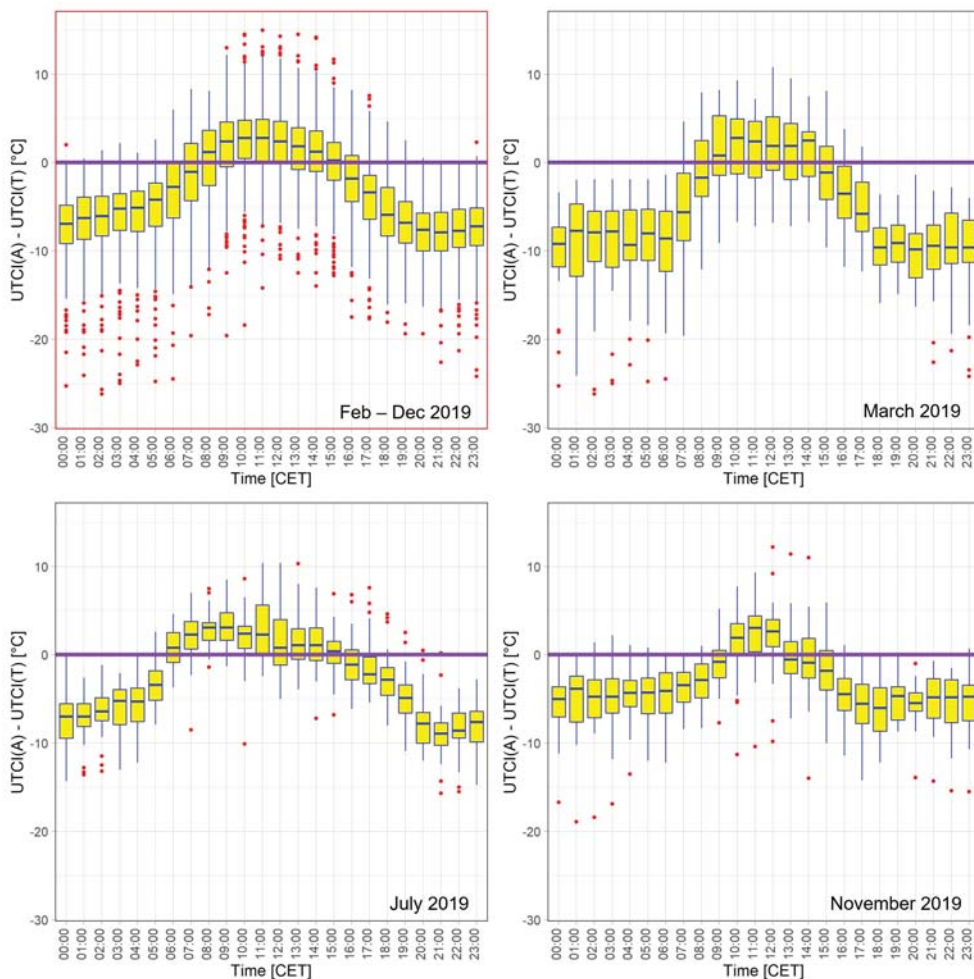


Figure 9. The daily course of differences between predicted [UTCI(A)] and calculated [UTCI(T) with $T_{mrt} = T$] UTCI values for period Feb-Dec 2019 (with red frame) and selected months from different seasons of 2019

values changes during the day, the model values are usually higher around noon.

This feature of the current ALADIN model calculation is probably determined by the T_{mrt} calculation solution. It is based on calculations of radiant fluxes of shortwave and long-wave radiation at the Earth's surface. Compared with the height of 1-1.5 meters, there is a significantly negative balance of long-wave radiation at night. Underestimating the UTCI model is the result of the computed T_{mrt} level.

The inaccuracy of the UTCI calculation is the second factor that influenced the test results. UTCI values were calculated without a directly determined T_{mrt} because radiant fluxes are not measured on AWS. Only the values of air temperature, relative humidity and wind speed at a height of 10 m were used for the calculation. The value T_{mrt} was determined equal to the air temperature.

Significant differences between the modelled and calculated UTCI values were the reason for looking for another

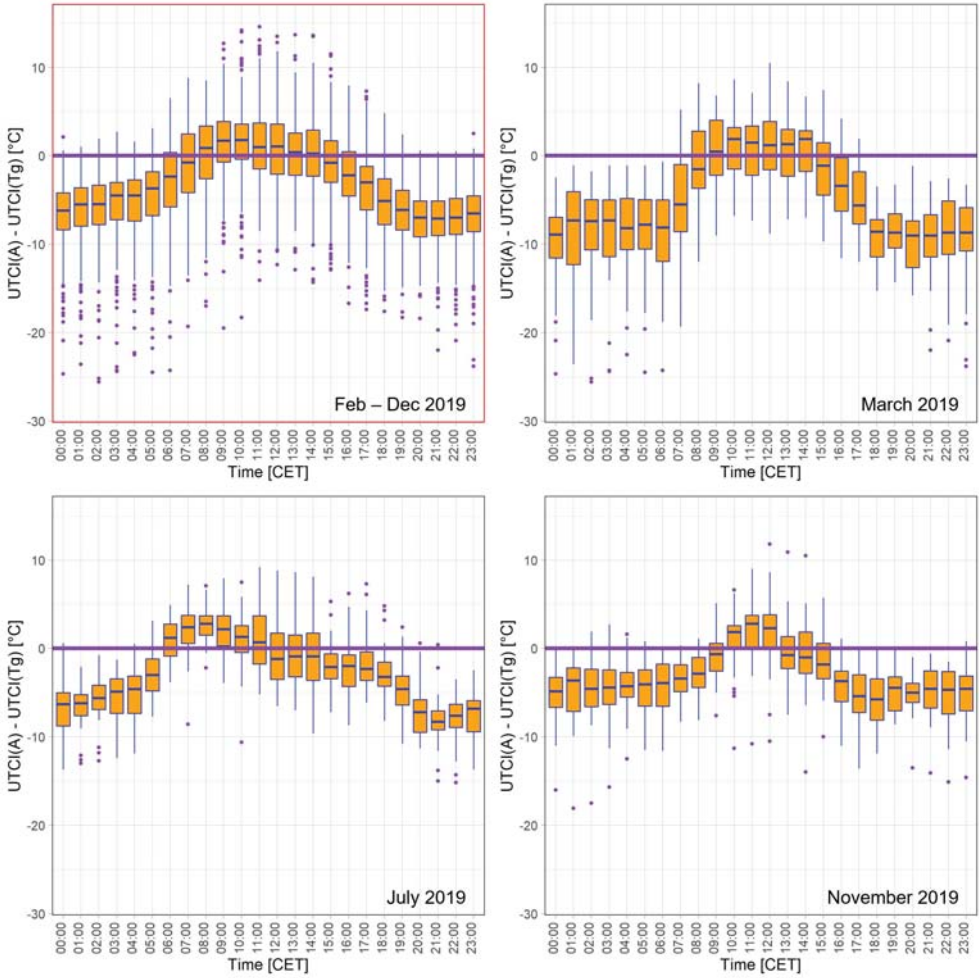


Figure 10. The daily course of differences between predicted [UTCI(A)] and calculated [UTCI(T_g) with T_{mrt} = T_g] UTCI values for period Feb – Dec 2019 (with red frame) and selected months from different seasons of 2019

T_{mrt} solution. The air temperature is also measured at a height of 5 cm (T_g – ground temperature). T_g values are more dependent on the radiation and heat balance of the surface. Therefore, T_g was chosen as a comparative value of T_{mrt}. The differences between the UTCI comparative value (T_{mrt} = T_g) and the UTCI predicted model are smaller, but insignificantly.

Properties of the studied location are the third reason why the differences between the predicted and the calculated UTCI values.

The Teplice weather station is located almost in the middle of the city with 50 thousand inhabitants. However, the influence of the surrounding buildings or the orientation of the streets and the distribution of urban greenery is below the resolution of the ALADIN model.

The findings of this work lead to the spread of tests to more locations. Negotiations with the CHMI Department of Numerical Weather Prediction will take place depending on the results of further tests.

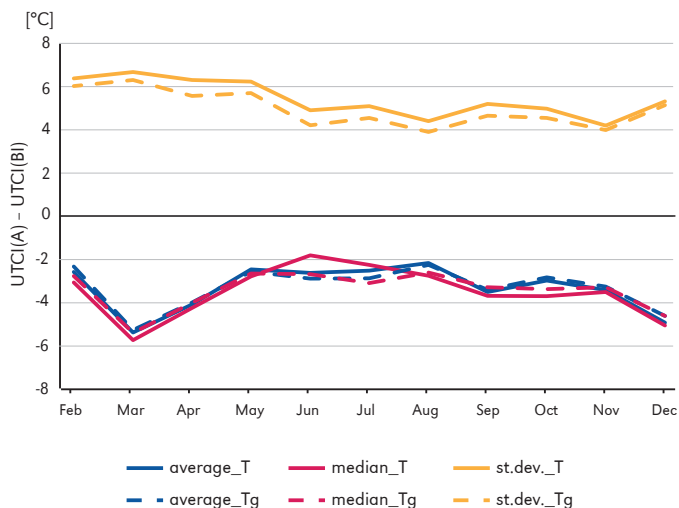


Figure 11. The annual course of difference between predicted [UTCI(A)] and calculated [UTCI(B)] UTCI values for 2019 (without January). The solid lines are for $T_{mrt} = T$, the two-dashed lines are for $T_{mrt} = T_g$

Acknowledgements

This work has been supported by the CHMI research project “Dlouhodobá koncepce rozvoje výzkumné organizace (DKRVO) Český hydrometeorologický ústav na období 2018-2022”, financed by the Czech Ministry of Environment.

I would like to thank Martin Hynčica for help with work in R software. I would also

thank to Radmila Brožková for preparing Figure 1 and advices on ALADIN model.

Editors' note:

Unless otherwise stated, the sources of tables and figures are the authors', on the basis of their own research.

References

- Andrade, H.C.C., Silva, A.B.C.G., Ribeiro, F.L.B., Wrobel, L.C. (2019). A parallel implementation of a thermoregulation model using the finite element method. *CILAMCE 2019: Proceedings of the XL Ibero-Latin-American Congress on Computational Methods in Engineering*, ABMEC. <http://bura.brunel.ac.uk/handle/2438/19922>
- Błażejczyk, K., Bröde, P., Fiala, D., Havenith, G., Holmér, I., Jendritzky, G., Kampmann, B. (2010). Nowy wskaźnik oceny obciążeń cieplnych człowieka. *Przegląd Geograficzny*, 82(1), 49-71. <https://doi.org/10.7163/PrzG.2010.1.2>
- Błażejczyk, K., Epstein, Y., Jendritzky, G., Staiger, H., Tinz, B. (2012). Comparison of UTCI to selected thermal indices. *International Journal of Biometeorology*, 56, 515-535. <https://doi.org/10.1007/s00484-011-0453-2>
- Chaudhuri, T., Soh, Y.C., Bose, S., Xie, L., Li, H. (2016). On assuming Mean Radiant Temperature equal to air temperature during PMV-based thermal comfort study in air-conditioned buildings. *IECON 2016-42nd Annual Conference of the IEEE Industrial Electronics Society*, Florence, 2016 (pp. 7065-7070). <https://doi.org/10.1109/IECON.2016.7793073>

- Fanger, P.O. (1972). *Thermal comfort: Analysis and applications in environmental engineering*, by P.O. Fanger. New York: McGraw-Hill Book Company
- Glossary of terms for thermal physiology (2003). *Journal of thermal biology*, 28(1), 75-106. [https://doi.org/10.1016/S0306-4565\(02\)00055-4](https://doi.org/10.1016/S0306-4565(02)00055-4)
- Gosling, S.N., Bryce, E.K., Dixon, P.G., Gabriel, P.M.A., Gosling, E.Y., Hanes, J.M., Hondula, D.M., Liang, L., Bustos Mac Lean, P.A., Muthers, S., Nascimento, S.C., Petralli, M., Vanos, J.K., Wanka, E.R. (2014). A glossary for biometeorology. *International Journal of Biometeorology*, 58, 277-308. <https://doi.org/10.1007/s00484-013-0729-9>
- Krüger, E.L., Minella, F.O., Matzarakis, A. (2014). Comparison of different methods of estimating the mean radiant temperature in outdoor thermal comfort studies. *International Journal of Biometeorology*, 58(8), 1727-1737. <https://doi.org/10.1007/s00484-013-0777-1>
- Lai, A., Maing, M., Ng, E. (2017). Observational studies of mean radiant temperature across different outdoor spaces under shaded conditions in densely built environment. *Building and Environment*, 114, 397-409. <https://doi.org/10.1016/j.buildenv.2016.12.034>
- Novák, M. (2013). Applications of the UTCI in the Czech Republic. *Geographia Polonica*, 86(1), 21-28. <https://doi.org/10.7163/GPol.2013.3>
- R Core Team. (2019). R: A language and environment for statistical computing. *R Foundation for Statistical Computing*, Vienna, Austria. <https://www.R-project.org/>
- Termonia, P., Fisher, C., Bazile, E., Bouyssel, F., Brožková, R., Bénard, P., Bochenek, B., Degrauwe, D., Derková, M., El Khatib, R., Hamdi, R., Mašek, J., Pottier, P., Pristov, N., Sity, Y., Smolíková, P., Španiel, O., Tudor, M., Wang ... Joly, A. (2018). The ALADIN System and its canonical model configurations AROME CY4T1 and ALARO CY40T1. *Geoscientific Model Development*, 11, 257-281. <https://doi.org/10.5194/gmd-11-257-2018>
- UTCI. (2012). Universal Thermal Climate Index. ReadMe_UTCI_a002.txt. *UTCI Universal Thermal Climate Index – Documents*. [online: 25 June 2012, cited: 6 June 2020]. http://www.utci.org/utci_doku.php
- Walikewitz, N., Jänicke, B., Langner, M., Meier, F., Endlicher, W. (2015). The difference between the mean radiant temperature and the air temperature within indoor environments: A case study during summer conditions. *Building and Environment*, 84, 151-161. <https://doi.org/10.1016/j.buildenv.2014.11.004>
- Wang, Y., Belluš, M., Ehrlich, A., Mile, M., Pristov, N., Smolíková, P., Španiel, O., Trojáčková, A., Brožková, R., Cedilnik, J., Klari, D., Kovai, T., Mašek, J., Meier, F., Szintai, B., Tascu, S., Vivoda, J., Wastl, C., Wittmann, T. (2018). 27 years of regional cooperation for limited area. Modelling in Central Europe (RC LACE). *Bulletin of the American Meteorological Society*, 99, 1415-1432. <https://doi.org/10.1175/BAMS-D-16-0321.1>
- Wickham, H. (2016). *ggplot2: Elegant Graphics for Data Analysis*. New York: Springer-Verlag. <https://doi.org/10.1007/978-0-387-98141-3>